



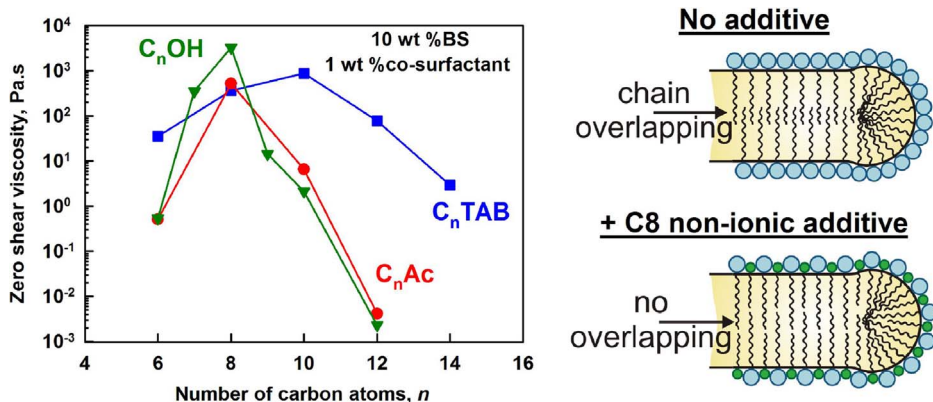
## Control of surfactant solution rheology using medium-chain cosurfactants



Z. Mitrinova, S. Tcholakova, N. Denkov\*

Department of Chemical and Pharmaceutical Engineering, Faculty of Chemistry and Pharmacy, Sofia University, 1 J. Bourchier Ave., 1164 Sofia, Bulgaria

## GRAPHICAL ABSTRACT



## ARTICLE INFO

## Keywords:

Surfactant rheology  
Wormlike micelles  
Cosurfactant  
Solution viscoelasticity  
Gel  
Fragrance  
Perfume

## ABSTRACT

The rheological properties of surfactant solutions play an important role in their applications. Here we study systematically how different cosurfactants affect the rheological properties of mixed solutions of the anionic surfactant sodium lauryl ether sulfate (SLES) and the zwitterionic cocoamidopropyl betaine (CAPB). Mixed SLES + CAPB solutions are used in various formulations due to their excellent foaming and cleaning properties. These solutions possess nearly Newtonian behavior and low viscosity. However, the addition of cosurfactants in low concentrations may significantly increase the viscosity of these solutions and even transform them into viscoelastic gels. Here we study systematically a wide range of ionic and nonionic cosurfactants with different head-groups, chain-lengths and structures of the hydrophobic tails (linear, branched, double bonded). We reveal an optimal chain-length of 8–10 carbon atoms of the cosurfactant molecules which ensures the highest viscoelasticity of the triple SLES + CAPB + cosurfactant solutions. Cationic cosurfactants and nonionic ones with small head-group (e.g. fatty alcohols and fatty acids) are most efficient in increasing the solution viscoelasticity. There is a hierarchy in the parameters of the cosurfactant molecules which govern this behavior – most important is the head-group charge, then the chain-length and, finally, the presence of branching and double bonds in the hydrophobic tails. The observed trends are explained with the effect of the cosurfactant molecules on the properties of the entangled wormlike micelles formed in these solutions.

\* Corresponding author.

E-mail address: [ND@LCPE.UNI-SOFIA.BG](mailto:ND@LCPE.UNI-SOFIA.BG) (N. Denkov).<http://dx.doi.org/10.1016/j.colsurfa.2017.10.018>

Received 11 August 2017; Received in revised form 2 October 2017; Accepted 7 October 2017

Available online 10 October 2017

0927-7757/ © 2017 Elsevier B.V. All rights reserved.

## 1. Introduction

Concentrated micellar solutions find applications in various industries and consumer products. Usually, there are specific requirements to their rheological properties, e.g. in dish-washing detergents and personal care products. One approach to control these properties is to ensure the formation of entangled wormlike micelles (WLM) which increase the solution viscosity and may even lead to the appearance of certain viscoelasticity of the solutions [1]. The micellar shape is governed primarily [2] by the packing parameter,  $p = v/(a_0 l_c)$ , which depends on the surfactant molecular characteristics: the molecule volume,  $v$ , the area-per-molecule,  $a_0$ , and the length of the hydrophobic tail,  $l_c$ . Increasing this parameter above  $p = 1/3$  leads to change in the micellar shape from spherical to rod-like and, eventually, to worm-like micelles with the related increase of solution viscosity and elasticity [3,4]. The theoretical models [5–11] which relate the micellar properties (such as shape, length and various relaxation times) with the overall rheological properties of the respective micellar solutions are briefly explained in Section 3 below and are used to interpret our experimental data.

There are several approaches to increase the packing parameter and to induce the formation of wormlike micelles. One possibility is to decrease the area of the surfactant head-group. With ionic surfactants this approach is often realized by adding electrolytes of high concentration [12,13]. The electrolytes screen the electrostatic repulsion between the head-groups of the neighboring molecules in the micelles and, thus, lead to the formation of more compact head-group arrangement on the micelle surface. Similar effect is observed when mixing oppositely charged ionic surfactants, e.g. cationic and anionic surfactants, or cationic/anionic with zwitterionic surfactants [14]. For ethoxylated nonionic surfactants, the area per head-group depends on the number of ethoxy groups in the surfactant head-group. For example, in the work of Acharya et al. [16] it is shown that there is an optimal number of EO groups which leads to highly viscous solutions of the SDS + C12EO3 mixture.

Another approach to vary the packing parameter is to increase the volume of the hydrocarbon fraction of the surfactant molecules. Well known examples are the double-tailed lipids which tend to form planar self-assembled structures due to the doubled volume,  $v$ , at (almost) fixed  $a_0$  and  $l_c$  [2].

Several papers studied the effect of cosurfactant chain-length on the micellar solutions of sucrose esters. Thus, Aramaki et al. [16] studied the effect of alcohol cosurfactants with chain-length varied between C3 and C9, on the viscosity of sucrose monohexadecanoate solutions, viz. for a main surfactant with C16 alkyl chain. They showed that the longer-chain alcohols are more efficient to increase the viscosity of such solutions. However, the cosurfactant chain-length was limited to 9 carbon atoms in these studies, because precipitates were formed and phase separation was observed at longer chain-lengths of the alcohols.

In a separate study [17], the same group analyzed the effect of fatty acids (FAC) with chain-length varied between C6 and C12. An optimal ratio between FAC and sucrose monopalmitate was observed and the highest viscosity was obtained when using fatty acids with 10 and 12 carbon atoms (C10Ac and C12Ac). In addition, these authors showed that changing the lauric acid into sodium laurate increases solution viscosity, due to electrostatic repulsion between the micelles and to the related “excluded volume” effect.

In another study, Raghavan et al. [18] showed for oppositely charged surfactants that the solution viscosity increases when increasing the asymmetry between the alkyl chains of sodium oleate (NaOA) and alkyltrimethylammonium bromide (CnTAB). The largest effect was observed for C8TAB. In Ref. [19], the effect of chain-length of various CnTABs on the micellar solutions of C16TAB was studied in the presence of KBr. The results showed that increasing the fraction of shorter-chain additive leads to lower solution viscosity, due to formation of micelles with shorter persistence length and higher flexibility. These results were explained with reduced van der Waals attraction

between the surfactant-cosurfactant tails with different lengths which, in turn, leads to less compact and less stable micelles.

Kamada et al. [20] studied the mixture of SDS + C12EO3 (as main surfactants) and found a maximum in the solution viscosity at a certain SDS to C12EO3 ratio. In the presence of cosurfactants (e.g., polar fragrance molecules) this maximum is shifted toward other ratios of the two main surfactants. These authors explained their results with solubilization of the polar cosurfactant molecules in the palisade layer, which changes the curvature of the micellar surface and, thus, shifts the surfactant ratio corresponding to maximum solution viscosity.

Parker and Fieber [12] studied the effect of cosurfactants (fragrances and other short- chained additives) on solution of SLES-2EO, in the presence of NaCl. In this system, a maximum in the viscosity is observed at a certain NaCl concentration. The authors showed that the addition of fragrance or oily cosurfactants can change the magnitude and/or the position of the viscosity maximum which is also explained with the solubilization of the cosurfactant molecules and the related change in the micelle flexibility (persistent length).

In our previous study [21] we reported that medium-chain fatty acids (C8 and C10 FAC) induce the formation of wormlike micelles when added to mixed surfactant solutions of SLES + CAPB. The triple solutions exhibit viscoelastic rheological response [21], while the double solutions of SLES + CAPB have low viscosity and (almost) Newtonian behavior. In contrast, the longer chain fatty acids (C12 to C18 FAC) have no such effect on solution rheology [21]. This phenomenon was explained with the mismatch between the hydrocarbon tails of the main surfactants (containing mainly C12 chains) and the cosurfactants with C8 or C10 tails. This mismatch seems to be essential for the formation of wormlike micelles, when cosurfactant is added in this system.

In an independent series of papers, Kralchevsky et al [22,23], observed a well pronounced peak in the solution viscoelasticity, when varying the concentration of the cosurfactants (fatty acids added to SLES + CAPB mixture) and used electron cryo-microscopy to clarify how the peak position and height are related to the transformations in the micellar shape and size.

The aim of the current paper is to study systematically how the cosurfactant molecular parameters affect the rheological behavior of SLES + CAPB solutions. We show that highly viscous and viscoelastic solutions could be formed by adding several classes of cosurfactants which differ substantially in their molecular characteristics. We observe a clear hierarchy in the parameters of the cosurfactant molecules which govern this rheological transition – most important is the cosurfactant head-group charge, followed by its chain-length and, finally, the presence of branching and double bonds in the hydrophobic tails. An optimal chain-length of 8–10 carbon atoms of the cosurfactant molecules is revealed, independently of the specific cosurfactant head-group, which ensures the highest viscoelasticity of the triple SLES + CAPB + cosurfactant solutions. These trends are explained by analyzing the effects of the cosurfactants on the properties of the wormlike micelles formed in these solutions.


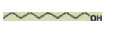
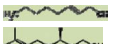
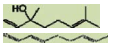
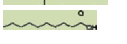

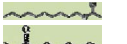
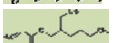

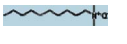
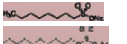
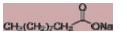

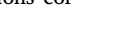
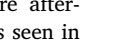
The paper is organized as follows: In Section 2 we describe the materials and methods used. In Section 3 we present the main experimental results. Their molecular interpretation is described in section 4. The main conclusions are summarized in section 5.

## 2. Materials and methods

### 2.1. Materials

The basic surfactant system, denoted hereafter as BS, is a mixture of sodium lauryl ether sulfate, SLES (product of Stepan Co., IL, USA, with commercial name STEOL CS-170, which contains around 1 EO group per molecule on average) and cocoamidopropyl betaine, CAPB (product of Goldschmidt, commercial name Tego Betaine F50). The concentration of the main surfactants in the studied solutions was 10 wt% of

**Table 1**  
Cosurfactants studied.

Name	Abbrev.	Head-group	Structure	Chain length	Surfact type	Compound type	Producer
Alkyl trimethyl ammonium bromide	C <sub>n</sub> TAB	N <sup>+</sup> (CH <sub>3</sub> ) <sub>3</sub> (Br) <sup>−</sup>		C <sub>6</sub> , C <sub>8</sub> , C <sub>10</sub> , C <sub>12</sub> , C <sub>14</sub>	cationic	Alkyl trimethyl ammonium bromide	Sigma-Aldrich
Fatty alcohols	C <sub>n</sub> OH	OH		C <sub>6</sub> , C <sub>7</sub> , C <sub>8</sub> , C <sub>9</sub> , C <sub>10</sub> , C <sub>12</sub>	nonionic	Alcohol	Sigma-Aldrich
3,7-dimethyl-6-octen-1-ol	C <sub>8</sub> OH_1 Citronellol			C <sub>8</sub>			
3,7-dimethyl-1,6-octadien-3-ol	Linalool			C <sub>8</sub>			
3,7-dimethyl-2,6-octadienal	Citral	CH <sub>2</sub> O		C <sub>8</sub>		Aldehyde	
Fatty acids	C <sub>n</sub> Ac	COOH		C <sub>6</sub> , C <sub>8</sub> , C <sub>10</sub> , C <sub>12</sub>		Organic acid	Fluka, TCI, Alfa Aesar
Octyl gallate	C <sub>8</sub> Gallate	OOCCH <sub>2</sub> (OH) <sub>3</sub>		C <sub>8</sub>		Ester	Sigma-Aldrich
Alkyl acetate	C <sub>n</sub> Acetate	OCOCH <sub>3</sub>		C <sub>6</sub> , C <sub>8</sub> , C <sub>10</sub>			
Methyl octanoate	C <sub>8</sub> Methyl	COOCH <sub>3</sub>		C <sub>8</sub>			
2-(ethylhexyl)-acrylate	EHA	OOCCHCH <sub>2</sub>		C <sub>6</sub>			Merck
Poly (ethylene glycol) octyl ether	C <sub>8</sub> PEG	[OCH <sub>2</sub> CH <sub>2</sub> ] <sub>n</sub> OH n = 2 + 9		C <sub>8</sub>		Ether	Sigma-Aldrich
N,N-dimethyldodecyl amine N-oxide	C <sub>10</sub> AO	N <sup>+</sup> - > O <sup>−</sup> (CH <sub>3</sub> ) <sub>2</sub>		C <sub>10</sub>	zwitterionic	Aminoxide	Sigma-Aldrich
Sodium octyl sulfonate	C <sub>8</sub> NaSO <sub>3</sub>	OSO <sub>2</sub> <sup>−</sup> Na <sup>+</sup>		C <sub>8</sub>	anionic	Alkyl sulfonate	Merck
Sodium alkyl sulfate	C <sub>n</sub> NaSO <sub>4</sub>	OSO <sub>3</sub> <sup>−</sup> Na <sup>+</sup>		C <sub>8</sub> , C <sub>10</sub>		Alkyl sulfate	
Sodium alkylate	NaAlkylate	COO <sup>−</sup> Na <sup>+</sup>		C <sub>8</sub> , C <sub>10</sub>		Sodium Carboxylate	TCI

SLES + CAPB, at fixed weight ratio of 2:1. These concentrations correspond to approx. 200 mM SLES and 100 mM CAPB.

Different cosurfactants with concentration of 1 wt% were afterwards solubilized in these 10 wt% SLES + CAPB solutions. As seen in Table 1, the studied cosurfactants differ by their charge (cationic, anionic, zwitterionic, nonionic), by the type of their hydrophilic head-group, and by the length, branching and double-bond presence in their hydrophobic chain. In one series of experiments, the cosurfactant concentration was varied, whereas the concentration of the main surfactants was still fixed at 10 wt%.

Most solutions were prepared by mild stirring at room temperature. The fatty acids and fatty alcohols with chain length between 8 and 12 carbon atoms, as well as the sodium alkyl sulfate, sodium octyl sulfonate, and octyl gallate were dissolved at 40 °C. The stirring continued until a homogeneous solution was obtained. These solutions were stored at room temperature for further studies and they remained homogeneous, without any visible phase separation or precipitation. Exceptions were the solutions of C8TAB and C8acetate with concentrations higher than 1 wt% and 70 mM, respectively, which were unstable upon long shelf-storage and precipitates were observed after ca. 2 months.

For measuring the trends in changing the micellar size and shape, in one series of experiments the concentrated solutions were diluted 20 times in de-ionized water (1 part of the stock solution of BS and 19 parts of de-ionized water) or in 112 mM NaCl solution. This particular electrolyte concentration was chosen because the used CAPB samples contains NaCl as admixture and the salt concentration is 112 mM NaCl for 100 mM CAPB [22].

All experiments were performed at 20 °C. The chemicals were used as received, without further purification.

## 2.2. Rheological properties of the surfactant solutions

The rheological properties of the surfactant solutions were characterized by Gemini rotational rheometer (Malvern Instruments, UK), using cone-and-plate geometry (diameter 20 mm and cone angle 4° or 0.07 rad), at 20 °C. The samples were kept between the rheometer plates for 5 min before each measurement to equilibrate the temperature. Two types of experiment were performed consecutively with each

sample. First, frequency sweep (dynamic experiment) was performed and the storage,  $G'$ , and loss,  $G''$ , moduli were measured, as functions of the frequency of oscillations, varied between 0.1 and 10 Hz, at fixed 2% amplitude of shear deformation. These measurements are in the linear viscoelastic regime, as determined previously by dynamic strain-sweep measurements. Second, a steady shear measurement was performed and the shear stress was measured as a function of the shear rate which was varied logarithmically between 0.01 and 300 s<sup>−1</sup>. At each shear rate, the plate was rotated for 5 s – the first 2 s were used to obtain a steady response, while the following 3 s were used to measure the mean shear stress. Control experiments confirmed that the results remain the same if these times are taken longer.

## 2.3. Viscosity of diluted surfactant solutions

Some of the studied solutions were diluted 20 times to check for the expected relation between the micelle size and solutions viscosity, see section 2.4. All diluted solutions were with Newtonian rheological behavior and relatively low viscosity. Their viscosity,  $\eta$ , was measured with thermostated capillary viscometer at 20 °C, after calibration with pure water.

## 2.4. Size determination by Dynamic light scattering

The dynamic light scattering (DLS) measurements of the micelle size were made with Malvern 4700C (Malvern Instruments, UK) gonio-metric light scattering system with a solid state laser (532 nm). The hydrodynamic diameter,  $d_h$ , of the micelles in the studied systems was determined from the measured micelle diffusion coefficient. The DLS experiments were performed at a measuring angle of 90°. Control measurements at 60° and 130° were also performed to confirm that the measured micelle size does not depend on the scattering angle. The signal analyzer was used in a multimodal regime and the volume averaged values are reported and analyzed in the current paper.

## 2.5. Optical microscope observations

Observations of the studied systems were performed with optical microscope Axioplan (Zeiss, Germany), equipped with a long-distance

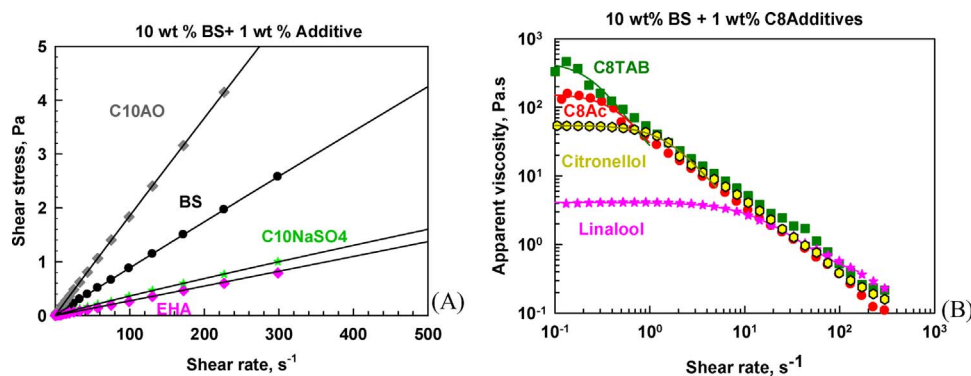


Fig. 1. (A) Shear stress as a function of the shear rate and (B) Apparent shear viscosity as a function of the shear rate for 10 wt% BS + 1 wt% cosurfactant solutions. Lines represent the theoretical description of the experimental data by eq. (1) or eq. (2), respectively. The referent BS system is shown with black circles in (A). All experiments are performed at  $T = 20^\circ\text{C}$ .

objective Zeiss Epiplan  $50\times/0.50$ . The system is equipped with a CCD camera, connected to a video-recorder and monitor. Small amount of the solution was placed between two glass slides and observed in regular transmitted or polarized light. In the latter experiments, the samples were observed by slowly rotating the second polarizer at relative angle between  $0^\circ$  and  $90^\circ$  to check for the possible presence of birefringent liquid crystalline phases.

### 3. Experimental results

#### 3.1. Typical rheological curves at steady shear

The 10 wt% SLES + CAPB solutions, containing different cosurfactants, exhibit a wide variety of rheological properties – from Newtonian to highly viscoelastic. The main surfactant system, SLES + CAPB without cosurfactant, exhibits Newtonian behavior in the studied range of shear rates and has a moderate viscosity of  $\approx 10$  mPa.s, see Fig. 1. The mixed SLES + CAPB solutions contain spherical and/or rod-like micelles, depending on the ratio and the total concentration of the two surfactants [24].

Some of the studied cosurfactants do not change qualitatively the rheological behavior of the solutions, Fig. 1A. For these systems a linear relation between the shear stress,  $\tau$ , and shear rate,  $\dot{\gamma}$ , is observed and can be used to determine the solution viscosity,  $\eta$ :

$$\tau = \eta \dot{\gamma} \quad (1)$$

In Fig. 1A we show illustrative experimental data for such systems, along with their fit by eq. 1.

Other cosurfactants increase the solution viscosity by several orders of magnitude and lead to non-Newtonian solution behavior, see Fig. 1B. For these systems, the dependence  $\eta$  vs.  $\dot{\gamma}$  consists of two well defined regions. At low shear rates the viscosity remains almost constant up to a given shear rate, followed by a steep viscosity decrease with the further increase of the shear rate. Remarkably, at high shear rates, all experimental curves merge around a single master line, with a slope very close to  $-1$ . At even higher shear rates these curves are expected to

level off at a constant value,  $\eta_\infty$ , but these rates were not reached in our experiments. Such shear thinning behavior is associated with the formation of entangled wormlike micelles in the solutions [17–18,25–29].

The first range, in which the viscosity remains constant, corresponds to the so-called “zero-shear viscosity”,  $\eta_0$ , which can be determined by fitting the experimental data with the Cross model [30] for the apparent solution viscosity vs. the shear rate,  $\dot{\gamma}$ :

$$\eta = \eta_\infty + \frac{\eta_0 - \eta_\infty}{1 + (K\dot{\gamma})^m} \quad (2)$$

Here  $\eta_0$  is the viscosity at  $\dot{\gamma} = 0$ ,  $\eta_\infty$  is the viscosity at  $\dot{\gamma} \rightarrow \infty$ ,  $m$  is a power-law index and  $K$  is consistency. Eq. (2) describes well the rheological curves for the systems with shear-thinning behavior and well-pronounced plateau region at low shear rates, see Fig. 1B. From the rheological curves in Fig. 1B we can determine  $\eta_0$ , to conclude that  $\eta_\infty < \eta_0$ , and to estimate that  $m \approx 1$  for all systems shown in this graph. The main differences between the various systems are in the values of  $\eta_0$  and  $K$ .

#### 3.2. Effect of cosurfactant concentration

To find an optimal concentration for studying the observed effects, we first varied the cosurfactant concentration for several systems which exhibit pronounced viscoelastic behavior. Four types of cosurfactants with C8 chain-length were compared: alcohol, fatty acid, acetate and trimethylammonium bromide, in the range between 0.1 and 3 wt%, see Fig. 2A. For all these systems we observed a clear maximum in the zero-shear viscosity at around 1 wt% of cosurfactant added. Similar maximum at around 1 wt% was observed with all cosurfactants for which such concentration dependence was studied (e.g. C10Ac, alcohols with various chain lengths).

For most of these cosurfactants 1 wt%  $\approx 70$  mM, viz. to around 4 times lower molar concentration than that of the main surfactants ( $\approx 300$  mM). Only for the cationic C8TAB, which has much larger molecular mass, the molar concentration is about twice lower,  $\approx 40$  mM. To check how important the molar ratio is in the studied

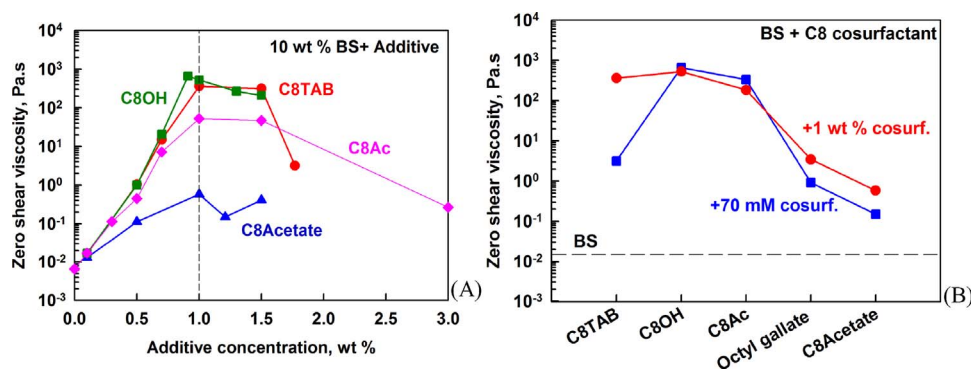


Fig. 2. (A) Zero shear viscosity, as a function of cosurfactant concentration for C8OH (green squares), C8TAB (red circles), C8Ac (pink diamonds), and C8Acetate (blue triangles) (B) Zero-shear viscosity for C8 cosurfactants with concentrations of 70 mM (blue squares) and 1 wt% (red circles). (For interpretation of the references to colour in this figure legend, the reader is referred to the web version of this article.)



surfactant mixtures, we performed a comparative series of experiments at fixed molar concentration of 70 mM cosurfactant, see Fig. 2B. One sees that the main experimental trends, with respect to the effect of cosurfactant head-group type, are the same for 1 wt% and for 70 mM solutions. The biggest difference for the two concentrations is observed with C<sub>8</sub>TAB – increasing the concentration of C<sub>8</sub>TAB from 1 wt% (36 mM) to 1.95 wt% (70 mM) leads to a two-fold decrease in  $\eta_0$ .

Based on the above results, in all further experiments, aimed to compare the cosurfactant effect on solution properties, we use 1 wt% cosurfactant in 10 wt% SLES + CAPB solution, because the studied effects are very well pronounced. Furthermore, the results shown in this section prove that the main observed effects are governed mostly by the cosurfactant molecular structure, while the cosurfactant concentration has a secondary effect, when the latter is maintained in the range between 1 and 1.5 wt%.

### 3.3. Effect of cosurfactant type on solution properties

#### 3.3.1. Solution appearance and cosurfactant solubility

Most of the initial solutions containing 1 wt% cosurfactant with chain-length between 6 and 10 carbon atoms were transparent. Exceptions were C8OH and C9OH which were slightly opalescent. Nevertheless, these solutions appeared homogeneous, without forming visible precipitates upon long-term shelf-storage. We studied the temperature dependence of these solutions and found that the BS + fatty alcohol solutions possess a cloud point (viz. appearance of visual opalescence upon temperature increase) – phenomenon which is typically associated with ethoxylated nonionic surfactants [31]. We determined the cloud points for SLES + CAPB solutions in presence of 1 wt% fatty alcohols to be  $\approx 8.5^\circ\text{C}$  for C8OH;  $\approx 16.5^\circ\text{C}$  for C9OH, and  $\approx 25.5^\circ\text{C}$  for C10OH. Note that the latter solution is transparent at the temperature of the rheological measurements,  $20^\circ\text{C}$ , whereas the other two solutions are opalescent at this temperature. Only a slight decrease in the concentration of C8OH, down to  $\approx 0.9$  wt%, led to the formation of clear, yet still very viscous solution at  $20^\circ\text{C}$ . Therefore, the solubility limit of C8OH in 10 wt% SLES + CAPB is  $0.95 \pm 0.05$  wt%, corresponding to  $\approx 74 \pm 4$  mM, and the observed effects are affected slightly by the formation of opalescent alcohol solutions.

For the longer (C12) chain-length cosurfactants we observed that the solutions containing 1 wt% C12OH were turbid at room temperature which is due to the limited solubility of this cosurfactant in the mixed SLES + CAPB micelles. The solutions containing C12Ac and C12TAB were transparent. Tzochcheva et al. [32,33] studied systematically the solubility of FAc and fatty alcohols in SLES + CAPB micelles and showed that, at a given cosurfactant chain-length, the micelles solubilize higher amount of FAc than fatty alcohol, due to more favorable interactions of the head-groups of the surfactant with the carboxylic group of the fatty acids.

All solutions were colorless, except for those containing Citral which appeared yellowish.

#### 3.3.2. Zero-shear viscosity and general rheological appearance

The effect of different cosurfactants with fixed concentration of 1 wt%, on the zero-shear viscosity of 10 wt% SLES + CAPB solutions, is compared in Fig. 3. The solutions are ordered in decreasing order of the respective viscosity value,  $\eta_0$ . One should note that for all systems between C<sub>10</sub>TAB and C<sub>14</sub>TAB the shear viscosity is determined according to Eq. (2), whereas the remaining systems have nearly Newtonian behavior and their viscosity is determined by Eq. (1). The highest value of  $\eta_0$  is measured with C<sub>10</sub>TAB as a cosurfactant, and it is almost 5 orders of magnitude higher ( $\approx 10^3$  Pa s) than the viscosity of the basic surfactant solution ( $\approx 0.01$  Pa s). On the other side, the lowest viscosity ( $\approx 2$  mPa s) is determined with C<sub>8</sub>NaSO<sub>4</sub> and it is approx. 5 times lower than that of the BS solution.

According to their rheological response, we divided these systems into three distinct groups (additional results from dynamic rheological

experiments which support this classification are presented in Section 3.3.3). The lists of cosurfactants which fall in each of these groups are shown in Table S1 in Supporting information.

The solutions with the highest values of  $\eta_0$  are viscoelastic gels with predominantly elastic response. These solutions do not flow in the time frame of minutes, even after applying small shear stress or under gravity. The bubbles which are captured in such gels float very slowly – days are needed for their travel under the effect of buoyancy, due to the very high apparent solution viscosity. The rheological measurements showed that the threshold value of  $\eta_0$  which governs the transition to such a gel-like behavior is around 100 Pa s.

The cosurfactants from the second group lead to formation of viscous solutions with a viscosity in the range between ca. 50 mPa.s and 100 Pa s. These solutions flow slowly under applied low shear stress or under gravity, see Fig. 3.

The third group of systems represents solutions with (almost) Newtonian behavior and viscosity which is lower than ca. 50 mPa.s.

#### 3.3.3. Shear moduli

Oscillatory measurements in shear deformation were performed with all systems between C<sub>10</sub>TAB and C<sub>10</sub>Acetate which belong to the groups of viscoelastic gels or highly viscous liquids (Groups 1 and 2). No results are shown for the low viscosity solutions (Group 3) as the rheometer sensitivity is too low for this type of measurements with such solutions.

In Fig. 4A we show illustrative results for BS + C<sub>8</sub>OH and BS + C<sub>8</sub>OH\_1 solutions. One sees that these solutions have viscoelastic behavior in the studied frequency range with prevailing loss modulus at low frequencies and higher storage modulus at higher frequencies. The intersection of  $G'(\omega)$  and  $G''(\omega)$  curves in the studied frequency interval gives information for the characteristic frequency,  $\omega_c$ , and the respective relaxation time of the micelle network,  $\tau_R = 1/\omega_c$ .

For the viscous liquids which have zero-shear viscosity lower than that of C<sub>8</sub>Gallate,  $G''(\omega) > G'(\omega)$  in the entire frequency range studied, viz. no crossing point between the curves was observed. Thus no characteristic relaxation time could be determined and these solutions are classified as predominantly viscous.

To compare the rheological behavior of the various systems, we plot in Fig. 5 the storage and loss moduli at a frequency of 1 Hz (for the respective complex moduli see Fig. S1 in Supplementary information). One sees that the gel systems in Group 1 have storage modulus which is higher than 100 Pa and which is higher by more than 3 times than the loss modulus. This result justifies our classification in which these solutions are considered as predominantly elastic. The systems in Group 2 have similar loss and storage moduli and for some of these systems the loss modulus is even higher than the storage modulus.

Note that our classification differs from the one proposed by Kumar et al. [34] where the gels are defined as elastic systems,  $G' > G''$ , in the entire frequency range from 0.01 to 10 rad s. The latter authors [34] use such more restrictive definition because the frequency independent elastic modulus implies lack of relaxation even at very long time scales. Our classification also makes sense in view of the wide variety of systems studied here and their applications.

Results for the characteristic relaxation time,  $\tau_R$ , for the various cosurfactants studied, are compared in Fig. 6 (see also Table 2). The relaxation time is directly related to the density of micelle entanglements and the time for their restructuring. The longest period is observed for the solutions defined as viscoelastic gels in our consideration (Group 1), for which this time is  $\geq 1$  s. One sees a positive correlation between  $\tau_R$  and  $\eta_0$  for the solutions from Groups 1 and 2, demonstrating that the more viscous samples have longer relaxation times of the micellar network which, in turn, leads to viscoelastic response of these solutions.

In the case of Maxwellian fluids, this positive correlation is reflected in a theoretically derived linear dependence between the zero-shear viscosity and the characteristic relaxation time  $\eta_0 = G_0\tau_R$ . Here  $G_0$  is

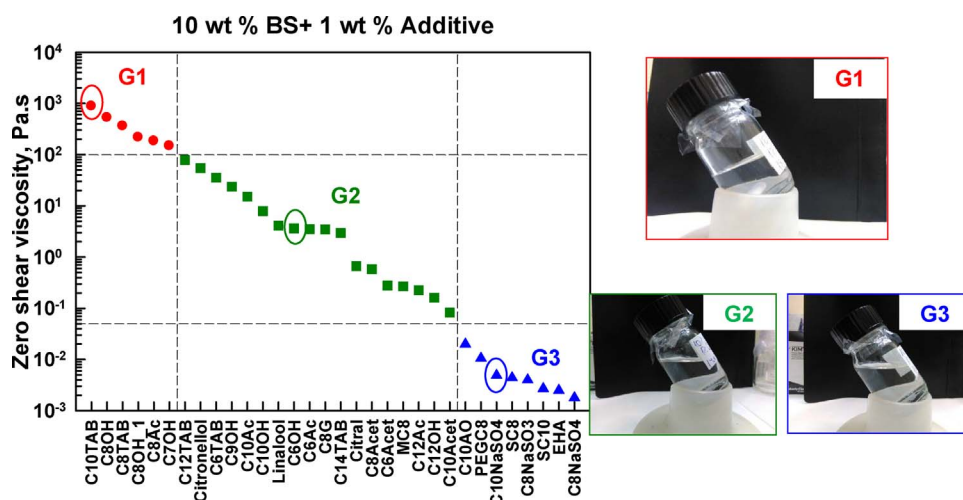


Fig. 3. Zero-shear viscosity,  $\eta_0$ , as a function of cosurfactant type for solutions of 10 wt% BS + 1 wt% cosurfactant. The viscosity of the referent BS system is 10 mPa.s. The vertical lines separate the three groups of solutions, as explained in the text. The horizontal dashed line indicates the viscosity of the referent SLES + CAPB solution, without any cosurfactant added. The pictures illustrate samples from the respective group, indicated by ellipses in the graph. All experiments are performed at 20 °C.

the so-called “plateau modulus”, viz. the elastic modulus extrapolated to infinite frequency. For all systems in Group 1 we found that  $G_0 > 100$  Pa. Thus, the zero-shear viscosity could be calculated also from the data obtained in the dynamic oscillatory experiments. We found that the values obtained from the two types of rheological experiments (steady and oscillatory shear) are in a very good agreement, within 3%, which supports the assumption that the viscoelastic properties of our solutions are governed by the characteristics of the wormlike micelles (WLM) present in these solutions [7].

For such solutions, the plateau modulus,  $G_0$ , brings information about the mesh size,  $\xi = (k_B T / G_0)^{1/3}$ , of the network of entangled WLM micelles [25]. The calculated mesh-size values for the systems, which exhibit measurable solution elasticity, are shown in Table 2 below. They are discussed in section 4 after presenting all other relevant parameters for these solutions.

The visco-elastic response of such entangled micellar solutions was explained and theoretically described by Cates [7–9], who considered two processes of stress relaxation – “reptation” and “reversible scission” of the micelles. At low oscillation frequency, these micellar solutions are predicted to obey Maxwell model, with single combined relaxation time [35]. At high oscillation frequencies, the rheological response of the wormlike micelles deviates from the Maxwell model, due to faster relaxation mode described by Rouse model [36].

To check whether our solutions have the characteristic rheological response of worm-like micelles, we plot the experimental data from the oscillatory experiments in the Cole-Cole plot, Fig. 7, showing the loss modulus as a function of the storage modulus [8]. Both moduli are plotted in dimensionless form, divided by  $G_c$ , which is the modulus at the crossing point of  $G'$  and  $G''$ . This plot shows that, indeed, at low frequencies all studied systems are described by a single relaxation time (the data lie on a semi-circle), whereas at high frequencies the experimental data deviate from the respective theoretical curve. This

deviation indicates the presence of wormlike micelles with multiple relaxation times.

From the experimental curves in Fig. 7 one can determine some characteristic times which include the contributions of two processes – reversible scission (breaking) of the micelles,  $\tau_{br}$ , and micelle reptation,  $\tau_{rep}$ . We used the numerical plots, calculated by Kern et al. [26], shown as continuous curves in Fig. 7, to determine numerically the ratio

$$\zeta = \tau_{br} / \tau_R \quad (3)$$

From the values of  $\zeta$  and  $\tau_R$ , determined as explained above, we could determine the characteristic time for micelle scission,  $\tau_{br}$ , see Table 2. For two of the systems, C<sub>10</sub>TAB and C<sub>8</sub>OH, we could determine also the reptation time using an additional relation [26],  $\tau_R = (\tau_{br} \tau_{rep})^{1/2}$ , which is valid only if  $\tau_{br} < \tau_{rep}$ . For all other systems, we found that  $\tau_{br} \geq \tau_{rep}$  and we cannot use this approach to determine  $\tau_{rep}$ .

These rheological results confirm the presence of wormlike micelles in the solutions studied – see e.g. Refs. [3,9,12] for extensive discussions of the specific rheological properties of such solutions. To exclude completely the possibility that some non-isotropic, liquid crystalline phases might be present in the solutions studied, we performed observations by optical microscopy in transmitted polarized light. All studied solutions were optically clear and isotropic, without any visible birefringent objects, and the variation of the angle between the polarizers did not reveal the existence of any textures that would indicate the presence of liquid crystals. Hence, we conclude that the rheological behavior of the studied solutions is governed entirely by the presence of isotropically distributed wormlike micelles.

We made various attempts to correlate the solution zero-shear viscosity,  $\eta_0$ , and the other rheological parameters with the cosurfactant partition coefficient,  $\log P$ , which reflects the polarity of cosurfactant molecules – see Section 4.2 for explanation of the procedure used. Such correlations are reported in previous studies [12] and could be

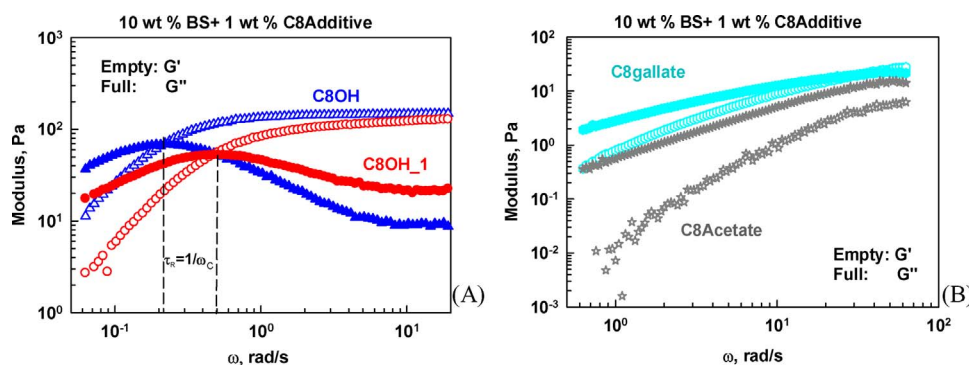


Fig. 4. Elastic and viscous moduli as functions of the deformation frequency for different systems. (A) Viscoelastic gels; (B) Viscous liquids.  $\omega_c$  is the frequency at which the elastic and viscous moduli are equal and  $\tau_R = 1/\omega_c$  is the characteristic relaxation time of the micelle network. All systems contain 10 wt% SLES + CAPB and 1 wt% cosurfactant; the measurements are performed at 20 °C.

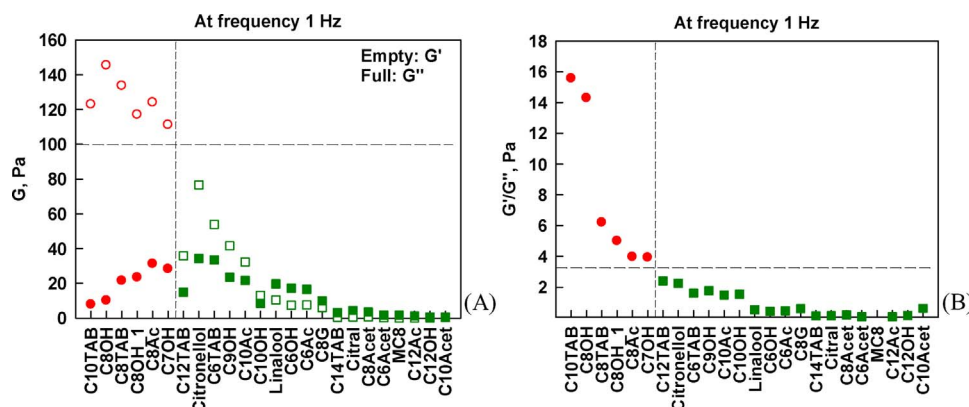


Fig. 5. (A) Elastic  $G'$  (empty symbols) and viscous,  $G''$  (full symbols) moduli, and (B) Ratio  $G'/G''$  for the various cosurfactants. The symbols denote gels (red circles) and viscous liquids (green squares), separated by a vertical line. All systems contain 10 wt% BS and 1 wt% cosurfactant. Experiments performed at a frequency of 1 Hz and temperature of 20 °C. (For interpretation of the references to colour in this figure legend, the reader is referred to the web version of this article.)

expected, as the molecular polarity affects the preferred cosurfactant localization in the mixed micelles – in the micelle core for the most hydrophobic ones, or in the palisade layer for the polar ones. However, all our attempts to find a simple clear correlation between the values of  $\log P$  and the solution rheological properties failed (see Section 4.2 for examples) which shows that other factors, beside the molecule polarity are also very important.

To clarify the effects of the various cosurfactant molecular parameters on the formation of wormlike micelles in the SLES + CAPB solutions, and on the respective solution rheological properties, we describe in the following sections the effects of the head-group type and of the tail length and structure.

### 3.4. Effect of cosurfactant chain-length on solution viscosity

In Fig. 8 we present the effect of cosurfactant chain-length on solution viscosity. In this series of cosurfactants we have included fatty alcohols, fatty acids, alkyl trimethyl ammonium bromides, and alkyl acetates, with chain-lengths varied between 6 and 14 carbon atoms. For all these classes of cosurfactants, we observed a sharp maximum in the apparent solution viscosity which appears at a specific chain-length of around 8–10 carbon atoms.

From Fig. 8A one sees that this maximum is at 8 carbon atoms for fatty alcohols, fatty acids, and alkyl acetates. The C8 fatty acids and alcohols are much more efficient in increasing the solution viscosity when compared to their C10 homologues. When the cosurfactant is with C12 tail and its chain-length is similar to the one of the main surfactants, no effect on the micelle size and on the solution rheological properties is observed. On the other side, C6 cosurfactants have the bigger molecular mismatch with the main surfactant, but their effect on viscosity is lower than that for C8 acids and alcohols. Thus we see that the molecular mismatch (optimal difference in the chain-length) is extremely important for the rheological behavior of the solutions studied.

Concerning the cationic cosurfactants CnTAB, one sees that all

studied chain-lengths, between C6 and C14, increase significantly the solution viscosity with a maximum observed at C10. In other words, the cationic surfactants are very efficient to increase the solution viscosity for a very wide range of chain-lengths, due to the strong electrostatic attraction with the main surfactant. Still, this effect is most pronounced around C8 to C10 chains – a result which shows that the chain-length mismatch is also important for this class of cosurfactants.

We conclude that cosurfactant chain-length of 8–10 carbon atoms is optimum for formation of long worm-like micelles, despite the fact that the tails of these cosurfactants are significantly shorter than the C12 tails of the main surfactants (SLES and CAPB). These trends are explained in section 4 below.

### 3.5. Effect of the double bonds and branching in the cosurfactant tail

Next, we analyzed the effect of the hydrocarbon chain structure on the solution viscosity, at fixed chain length of 8 carbon atoms. For this purpose, in Fig. 8B we compare the zero-shear viscosity of solutions containing C<sub>8</sub>OH, C<sub>8</sub>OH\_1, Citronellol, Linalool and Citral as cosurfactants. One sees that the solution viscosity decreases significantly with the increase of the number of double bonds and with branching in the cosurfactant molecules.

### 3.6. Effect of the cosurfactant head-group

In Fig. 9 we compare the results obtained with BS solutions, containing cosurfactants with 6, 8, 10 and 12 carbon atoms in their tails, for several types of cosurfactant head-groups. Results for cationic, nonionic (alcohols, fatty acids, esters) and anionic cosurfactants are shown in the order of viscosity decrease. One sees similar trends for all chain-lengths studied. The highest viscosity is observed for the cationic cosurfactants and the alcohols, whereas the lowest viscosities are measured with the anionic cosurfactant.

The observed trends could be explained with two different effects. In the case of the CnTAB, strong electrostatic attraction occurs between

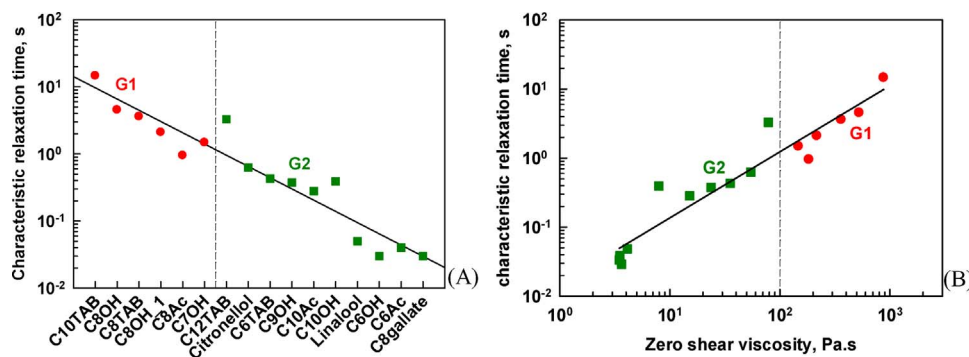


Fig. 6. Characteristic relaxation time,  $\tau_R$ , as a function of (A) system type and (B) zero shear viscosity. All systems contained 10 wt% BS and 1 wt% additive. All experiments are performed at  $T = 20$  °C. The vertical lines separate the surfactants in Groups 1 and 2.

**Table 2**

Values of the zero-shear viscosity,  $\eta_0$ , characteristic frequency,  $\omega_c$ , relaxation time,  $\tau_R$ , plateau modulus,  $G_0$ , mesh size of the micelle network,  $\xi$ , minimum in the viscous modulus as a function of frequency,  $G_m''$ , number of entanglement points per micelle,  $n_{ent}$ , micelle breakage time,  $\tau_{br}$ , and micelle reptation time,  $\tau_{rep}$ , for the various chemical classes of cosurfactants. The data, corresponding to a maximum in the values of  $\eta_0$  for a given class of cosurfactant, are shown in bold.

Cosurfactant	$\eta_0$ [Pa s]	$\omega_c$ [rad s <sup>-1</sup> ]	$\tau_R$ [s]	$G_0$ [Pa]	$\xi$ [nm]	$G_m''$ [Pa]	$n_{ent}$	$\tau_{br}$ [s]	
C <sub>6</sub> TAB	26.5	2.3	0.43	61.3	40.4	33.2	1.8	4.4	< 4.4
C <sub>8</sub> TAB	408	0.3	3.6	113.1	32.9	17.3	6.5	4.4	< 4.4
<b>C<sub>10</sub>TAB</b>	<b>1750</b>	<b>0.1</b>	<b>14.61</b>	<b>119.5</b>	<b>32.3</b>	<b>8.0</b>	<b>15</b>	<b>5.6</b>	<b>38.4</b>
C <sub>12</sub> TAB	80.6	0.3	3.30	22.4	56.5	11.8	1.9	16.6	< 17
C <sub>6</sub> OH	2.0	34.3	0.03	70.0	38.7	–	–	0.3	< 0.3
C <sub>7</sub> OH	151	0.7	1.48	101.5	34.1	<b>25.8</b>	<b>3.9</b>	1.8	< 1.8
<b>C<sub>8</sub>OH</b>	<b>640</b>	<b>0.2</b>	<b>4.54</b>	<b>141.0</b>	<b>30.6</b>	<b>9.0</b>	<b>16</b>	<b>1.7</b>	<b>11.9</b>
C <sub>9</sub> OH	18.4	2.7	0.38	48.9	43.6	20.4	2.4	1.7	< 1.7
C <sub>10</sub> OH	6.3	2.5	0.39	16.0	63.2	13.6	1.1	1.8	< 1.8
C <sub>6</sub> Ac	2.3	26.0	0.04	58.6	41.0	–	–	0.4	< 0.4
<b>C<sub>8</sub>Ac</b>	<b>124</b>	<b>1.1</b>	<b>0.95</b>	<b>130.3</b>	<b>31.4</b>	<b>18.4</b>	<b>7.1</b>	<b>1.2</b>	<b>&lt; 1.2</b>
C <sub>10</sub> Ac	12.5	3.5	0.28	43.8	45.2	18.1	2.4	1.3	< 1.3
<b>C<sub>8</sub>OH_1</b>	223	0.5	2.11	105.8	33.7	21.2	5.0	2.6	
Citronellol	50.1	1.6	0.63	79.7	37.0	32.7	2.4	2.9	–
Linalool	2.8	20.6	0.05	58.5	41.0	–	–	0.5	–
Octyl gall	1.2	29.8	0.03	38.7	47	–	–	0.3	–

the main anionic surfactant SLES and the cationic cosurfactant molecules. This is a known effect in literature, related to a decreased repulsion between the head-groups and closer packing inside the surface layer of the mixed micelles. Effectively, this corresponds to reduced area-per-molecule and increased packing parameter [2]. As a result, wormlike micelles are formed upon addition of the cationic cosurfactant.

On the other hand, the nonionic cosurfactants with small head-groups (fatty alcohols, fatty acids [37] at the studied pH  $\approx 6$ ) could also enhance significantly the packing in the surface layer of the mixed micelles, because the cosurfactant molecules are able to fill the gaps and displace water between the surfactant molecules. In agreement with this explanation, the increase in the head-group size of the nonionic cosurfactant (e.g. methyl acetate) leads to much smaller effect on the solution viscosity. Therefore, for the nonionic cosurfactants the small head-group size is very important for observing strong effects.

To quantify the latter explanation, in Fig. 9B we show the molecular structures of the nonionic surfactants studied (fatty acid, alcohol, and acetate) with chain-length of 8 carbon atoms, optimized with the Chem 3D office package. One sees that the molecule with the lowest excluded head-group area is C<sub>8</sub>OH (18.9 Å<sup>2</sup>) which is very close to the cross-sectional area of the hydrocarbon chain (18.9 Å<sup>2</sup>), followed by the fatty acid (22.3 Å<sup>2</sup>) and the acetate (25.2 Å<sup>2</sup>). This comparison confirms that the nonionic cosurfactant molecules with the smallest area-per-head-group leads to the most significant effect on solution viscosity, presumably due to the better packing of the head-groups on the surface of the mixed micelles. The significantly smaller effect of octyl acetate indicates that there is a threshold area-per-molecule of the cosurfactant (around  $23 \pm 1$  Å<sup>2</sup>) above which the viscosity decreases by two orders

of magnitude.

Note that the cationic CnTABs cosurfactants have rather voluminous head-group and still have strong effect on solution viscosity. Thus we conclude that the effects of the cationic and nonionic cosurfactants are related to different packing in the mixed micelles. Nevertheless, both effects are comparable in magnitude and are most pronounced at 8–10 carbon atoms in the cosurfactant tails. Further discussion on the differences between CnTAB and the nonionic surfactants is presented in Section 4.

In the system with anionic cosurfactants, there is a prevailing electrostatic repulsion between the molecules of the cosurfactant and SLES in the mixed micelles. This leads to larger average area-per-molecule and lower packing parameter, compared to the referent system without cosurfactant. Hence, the micelle size is reduced and the viscosity decreases when compared to the reference SLES + CAPB solution, as expected.

### 3.7. Properties of diluted solutions

To check for the expected relation between the micelle size and solution viscosity, we performed additional experiments after diluting the original 10 wt% solutions. This dilution was necessary, as the micelle size could not be determined in the original solutions by dynamic light scattering (DLS) – most of these solutions were too viscous.

The micelle size was analyzed for the surfactant mixtures containing C8 cosurfactants, used to construct Fig. 9. The original solutions were diluted 20 times either with water or with 112 mM NaCl solution. The latter concentration was chosen, as previous studies [22] showed that 10 wt% SLES + CAPB solution contains also 112 mM NaCl, introduced

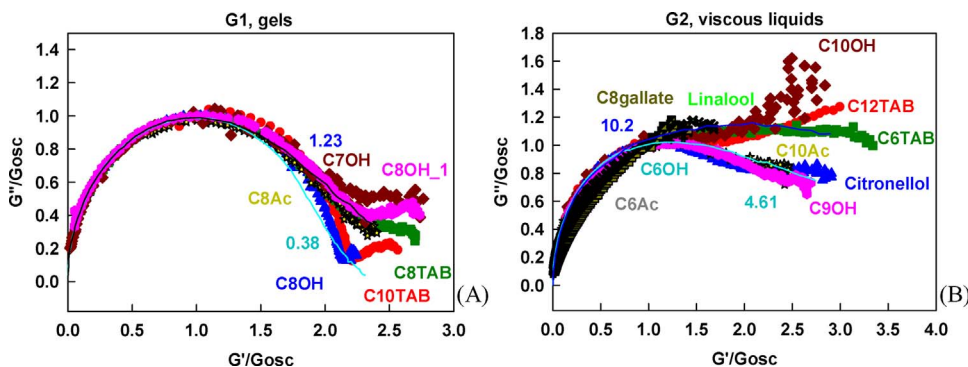


Fig. 7. Cole-Cole plot for 10 wt% BS + 1 wt% cosurfactant for the solutions behaving as (A) gels or (B) viscous liquids. The continuous theoretical curves represent numerical results, calculated in Ref. [15], and the numbers indicate the ratio  $\tau_{br}/\tau_R$  (see Eq. (3)).



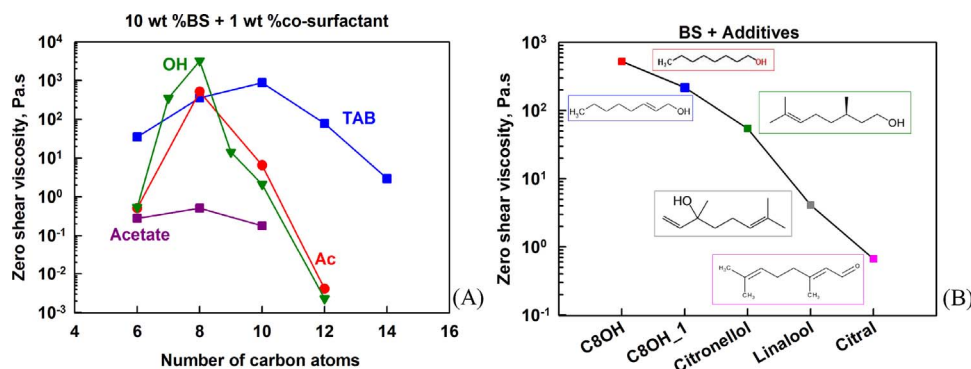


Fig. 8. (A) Zero-shear viscosity as a function of cosurfactant chain lengths for TABs (blue squares), alcohols (green triangles), fatty acids (red circles) and acetates (purple squares). (B) Zero-shear viscosity for several cosurfactants which all have a chain-length of 8 carbon atoms and small head-group (alcohol or aldehyde). The results are shown in the order of increasing number of double bonds and branching in the cosurfactant molecules. (For interpretation of the references to colour in this figure legend, the reader is referred to the web version of this article.)

with the CAPB. Thus we could clarify whether the electrolyte, introduced with the CAPB in the mixed surfactant solutions, plays a role in the micelle structure and in the solution rheological properties.

One can see in Fig. 10 that all solutions diluted with deionized water contain small spherical micelles with diameter between 3 and 5 nm. In contrast, dilution with 112 mM NaCl solution results in well pronounced differences between the solutions studied. The cationic cosurfactant gives the largest micelle size, in agreement with the observed highest viscoelasticity of the respective concentrated solutions. The order of micellar size decrease in the solutions, diluted with NaCl, is the same as for the decrease of  $\eta_0$  of the concentrated solutions. There is also a reasonable correlation between the viscosity of the diluted solutions and the respective micelle size, as expected (Fig. 10B).

Thus we conclude from these experiments that: (1) the electrolyte, introduced with CAPB in these systems, plays an important role in the micelle size and solution viscosity; (2) the high viscoelasticity and viscosity of the concentrated solutions reflect the largest size of the respective mixed micelles; and (3) the main role of the cosurfactants is to induce the formation of entangled worm-like micelles with long relaxation times.

## 4. Discussion

### 4.1. Relation between micelle properties and solution viscoelasticity

To understand better the origin of the variations in the viscoelastic properties of the solutions studied, in the current section we analyze the properties of the worm-like micelles. Their characteristics, as determined from the rheological measurements, are summarized in Table 2 where they are grouped according to the type of the cosurfactant head-group. In Table S2 in the Supplementary materials we show the same data, in the order of descending values of the zero-shear viscosity of the solutions.

Along with the values, calculated as explained in Section 3, in Table 2 and S2 we include data for the minimum in the curves  $G''(\omega)$

which is denoted as  $G_m''$ , and of the number of entanglement points per micelle,  $n_{ent} \approx G_0/G_m''$  (see Fig. 11 for illustration and Ref. [38] for explanations of the latter estimate).

One sees from Table 2 that the maxima in  $\eta_0$  and  $G_0$  (for a given class of cosurfactant) are related to clear maxima in the following characteristics of the micelles – relaxation time,  $\tau_R$ , reptation time,  $\tau_{rep}$ , and number of entanglement points,  $n_{ent}$ , see Fig. 12 for illustrative results. All these parameters are interrelated, and the observed maximum values correspond to longest entangled micelles for the given class of cosurfactants. Just as examples, the number of entanglement points is proportional to the micelle length,  $n_{ent} \propto L$ , and the reptation time is proportional to the cube of micelle length,  $\tau_{rep} \propto L^3$ . Therefore, we conclude that the observed viscoelastic behavior is governed exclusively by the length of the entangled micelles,  $L$ , and the related number of entanglement points per micelle,  $n_{ent}$ . From these data we can deduce also that viscoelastic solutions (Group 1) are formed when  $n_{ent} > 5$ , whereas highly viscous solutions (Group 2) are in the range of approx.  $3 < n_{ent} < 5$ . Only for the micelles with  $n_{ent} > 10$  we could determine the reptation time,  $\tau_{rep}$ , as the micelles are so long that  $\tau_{rep} > \tau_{br}$ .

Interestingly, for a given class of cosurfactant, we do not observe a maximum in the estimated micelle breakage time,  $\tau_{br}$ . For the shortest chain-lengths alcohols and fatty acids,  $C_6OH$  and  $C_6Ac$ , we observe systematically smaller values of  $\tau_{br}$ . This result shows that the excessive mismatch in the chain-lengths of the main surfactants and the cosurfactant, for  $C_6OH$  and  $C_6Ac$ , reduces the cohesion energy between the molecules in the micelles, thus facilitating micelle breakage. Indeed, as discussed in Ref. [2], the molar cohesive energy between alkyl chains in bulk alkanes increases by  $\approx 6.9 \text{ kJ mol}^{-1}$  per one  $-CH_2-$  group. For the longer chain-length alcohols and acids,  $C_7$  to  $C_{10}$ , as well as for  $C_6TAB$  to  $C_{10}TAB$  cosurfactants, the values of  $\tau_{br}$  are almost the same within a given class of cosurfactant. Thus we conclude that the variations in the values of  $\tau_{br}$  could not be used to explain the observed variations in  $\eta_0$  and  $G_0$ . On the other hand, the values of  $\tau_{br}$  for  $C_nTAB$ s are systematically longer than those of the other classes of cosurfactants

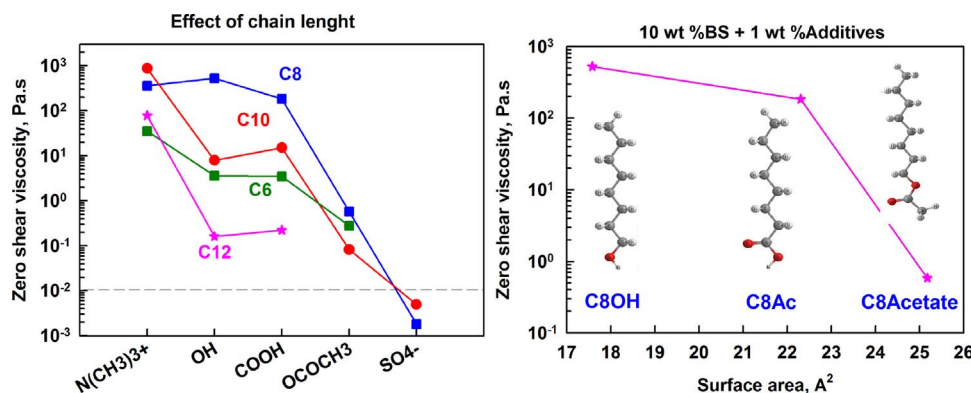


Fig. 9. Zero-shear viscosity as a function of (A) cosurfactant head-group type for different chain-lengths: C6 (green squares), C8 (blue squares), C10 (red circles); and C12 (pink stars); (B) head-group area for the nonionic C8OH, C8Ac and C8Acetate. (For interpretation of the references to colour in this figure legend, the reader is referred to the web version of this article.)

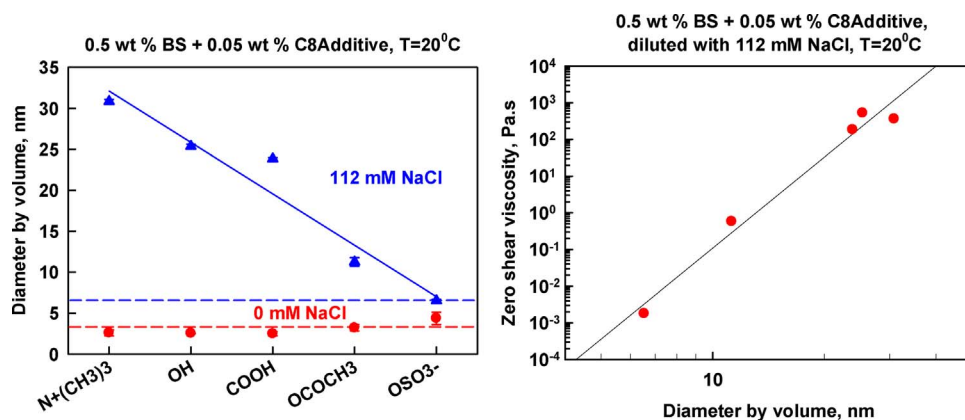


Fig. 10. (A) Micelle diameter for cosurfactants with C8 chain-length and different head-groups. The red circles are for dilution with deionized water, whereas the blue triangles are for dilution with 112 mM NaCl. (B) Zero-shear viscosity of the concentrated solutions vs. the micelle size in solutions diluted with 112 mM NaCl. The horizontal lines in (A) indicate the size of the SLES + CAPB micelles, without cosurfactant; the curve in (B) is guide to the eye. (For interpretation of the references to colour in this figure legend, the reader is referred to the web version of this article.)

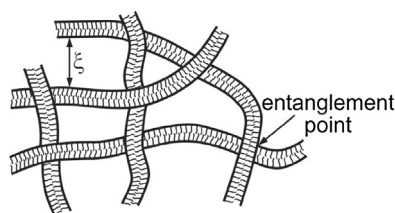


Fig. 11. Illustrative presentation of the micellar network, formed from entangled worm-like micelles. Upon applied stress, the micelles could relax either via diffusion within this network (reptation) or via micelle scission (breakage) at the entanglement points and subsequent reforming which eliminates these points.

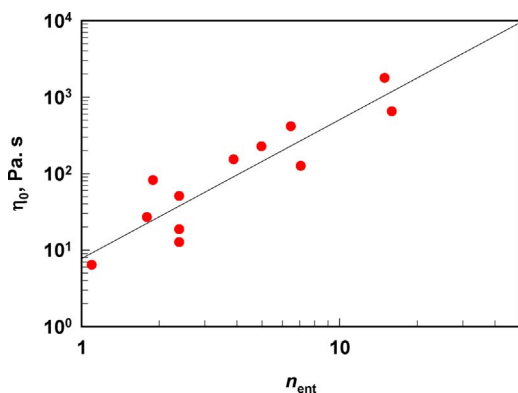


Fig. 12. Correlation plots for the zero-shear viscosity of the surfactant solutions and the number of entanglement points of the micelles in these solutions.

which is reflected in the higher values of  $\eta_0$  and  $G_0$  for this class of cosurfactants (see Fig. 8A). This comparison indicates that the electrostatic attraction between the cationic TAB head-group and the anionic SLES increases the molecular cohesion within the micelles,

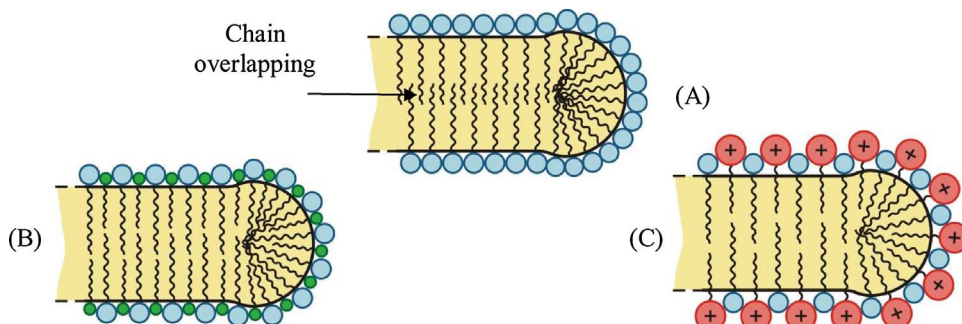


Fig. 13. Schematic presentation of the most probable mechanism by which C8-C10 cosurfactants increase the end-cap energy,  $\varepsilon_{ec}$ . (A) Reference system in which the C12 tails of the main surfactant molecules overlap severely both in the cylindrical body and in the spherical end-cap regions of the micelles; (B) The nonionic cosurfactants with small head-group and C8 tails fit between the main surfactant molecules and reduce significantly the tail overcrowding in the center of the cylindrical body of the micelles, thus increasing the energy for end-cap creation; (C) The cationic cosurfactants act in a similar mode, however, due to their larger head-groups and electrostatic attraction with the anionic surfactant, they sit on top of the head-groups layer of the main surfactant molecules.

For simplicity, the two main surfactants (SLES and CAPB) are not distinguished and their charges are not displayed in the figure.

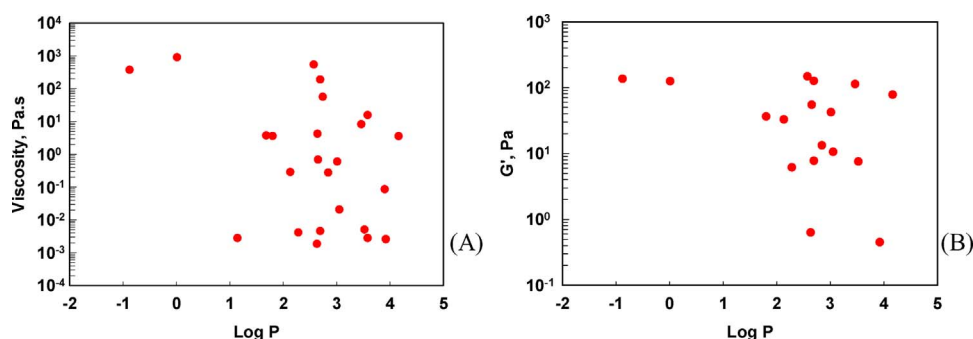


Fig. 14. Correlation plots of  $\eta_0$  and  $G'$  vs.  $\log P$  for the cosurfactants studied.

the cylindrical body of the micelles, as evidenced by the shorter relaxation times for these cosurfactants. Indeed, if the inclusion of the cosurfactant molecules with C8-C10 tails leads to better packing-stress relaxation in the cylindrical body of the micelles, as compared to the spherical end-caps, then the cosurfactants will reduce the energy of the cylindrical part and will thus increase the energy difference between the spherical and the cylindrical regions, viz. the values of  $\varepsilon_{ec}$  (see Fig. 13B,C for schematic illustration of this explanation). Thus we explain the effect of the C8-C10 cosurfactants with an optimal chain packing in the cylindrical region of the micelles which reduces the energy of this region.

Note that the packing of the small head-group and large head-group cosurfactants in the mixed micelles is different (cf. Fig. 13B and C). The small head-groups of the fatty acids and fatty alcohols are known to fit well in between the head-groups of the main surfactants, Fig. 13B, as a result of strong hydrogen bonding and inter-tail hydrophobic attraction [21,32,33,37]. The large head-groups of the  $C_n$ TAB do not allow these cosurfactants to fit in the space between the heads of the main surfactant molecules. Instead, one could expect that the TAB head-groups lay over the plane in which the head-groups of the main surfactants are located, as shown in Fig. 13C. The strong electrostatic attraction between the oppositely charged head-groups of  $C_n$ TAB and SLES stabilizes this configuration. This difference in the cosurfactant arrangement could explain the maximum at longer C10 tail for  $C_n$ TAB cosurfactants, as compared to the optimal C8 tail for fatty alcohols and acids. Indeed, the size of the head-groups of the main surfactants is comparable to the chain-length of a fragment of two neighboring  $-\text{CH}_2-$  groups ( $\approx 0.25$  nm).

On the other hand,  $\tau_{br}$  depends on the activation energy for end-cap formation,  $\varepsilon^\ddagger$ , and the micelle length via the expression [7,12]:

$$\tau_{br} \propto L^{-1} \exp\left[\frac{\varepsilon^\ddagger}{kT}\right] \propto \exp\left[\frac{(\varepsilon^\ddagger - 2\varepsilon_{ec})}{kT}\right]$$

The fact that  $\tau_{br}$  remains almost constant within a given class of cosurfactant, as discussed above, shows that the variations in  $\varepsilon_{ec}$  and  $\varepsilon^\ddagger$  are highly correlated – the increase of  $\varepsilon_{ec}$  is related to similar increase in  $\varepsilon^\ddagger$  and vice versa.

Such correlations between equilibrium and transition states are well known in physical organic chemistry and are used when considering the kinetics of organic reactions. They are generally termed as “linear free energy relationships” and popular examples are the Hammett equation and Taft equation [40,41]. Furthermore, the existence of such correlation means that there is a close structural similarity between the highest energy transition state before micelle scission (breakage) and the final state of the broken micelle. In other words, the energy maximum in the process of micelle breakage, expressed via  $\varepsilon^\ddagger$ , appears in the latest stages of the breakage process when the two end-caps with energy  $2\varepsilon_{ec}$  are forming.

#### 4.2. Lack of direct correlation between the polarity of cosurfactant molecules and solution viscoelastic properties

At the end, let us prove our statement that there is no simple direct correlation between the cosurfactant effect on the solution viscoelasticity and the polarity of the cosurfactant molecules, characterized by their  $\log P$  parameter. By definition, this parameter is determined from the ratio of the solubilities of the respective substance in octanol and in water:

$$\log_{10} P = \frac{[C]_{\text{in octanol, mol/l}}}{[C]_{\text{in water, mol/l}}} \quad (4)$$

We calculated  $\log P$  for the various cosurfactants using the free chemical structure database ChemSpider© (Royal Society of Chemistry 2015) and the software package ChemAxon which is based on the QSAR approach.

The results for  $\log P$  showed that most of the studied cosurfactants are predominantly hydrophobic, with a partition coefficient greater than 2. This means that the cosurfactants have low solubility in water and are predominantly incorporated inside the micelles. The only negative coefficients are those for C6TAB ( $\log P = -1.76$ ) and C8TAB ( $\log P = -0.87$ ), meaning that these molecules are more soluble in the aqueous phase than in octanol, due to the charged quaternary ammonium ion in their head-group and the relatively short hydrophobic chain. Nevertheless, these molecules have a very strong effect on the solution rheological properties which is a clear indication that their positive charge enhances the cosurfactant incorporation inside the micelles, in line with the discussion in Section 4.1.

Illustrative correlation plot between the values of  $\eta_0$  and  $\log P$  is shown in Fig. 14. One sees that the data for a given class of surfactant show a maximum viscosity at a given intermediate value of  $\log P$ . However, the data for the different classes of surfactants do not group around a single master curve. This lack of direct correlation is not surprising, because we observe strong effects on the micelle properties of molecules with very different polarities (e.g. C6TAB with  $\log P = -1.76$  and C8OH with  $\log P = +2.58$ ).

Note that no such wide range of cosurfactants has been reported until now in the literature – limited correlations are seen for similar in head-group cosurfactants but these correlations cannot be generalized for a wider set of chemical structures.

## 5. Conclusions

We studied systematically the effect of cosurfactants with various molecular structures on the rheological properties of SLES + CAPB solutions. According to their rheological behavior, all studied solutions could be divided into three groups:

- Viscoelastic gels, characterized with high zero-shear viscosity,  $\eta_0 > 100$  Pa s, shear elastic modulus,  $G' > 100$  Pa, and ratio  $G'/G'' > 3$  (at frequency 1 Hz);
- Viscous liquids with zero-shear viscosity between 0.05 Pa s and



100 Pa s, and with similar values of  $G'$  and  $G''$ ;

- Liquids with Newtonian rheological behavior and viscosity  $< 0.05$  Pa s.

There is a clear hierarchy in the parameters of the cosurfactant molecules which affect the rheological behavior of these solutions:

- Most important are the head-group charge and the alkyl chain-length, followed by the presence of branching and double bonds in the hydrophobic tails.
- For the same head-group, highest viscosity is observed with cosurfactants with chain-length of 8–10 carbon atoms.
- At given tail, highest viscoelasticity is observed with positively charged cosurfactants and with nonionic cosurfactants having small head-groups.
- Increasing number of double bonds and/or branching of the cosurfactant tails leads to lower solution viscosity.
- No simple correlation trend was found between solution rheological properties and any single property of the cosurfactant molecules (e.g.,  $\log P$ ).

The observed trends are analyzed by considering the properties of the entangled wormlike micelles, formed in these solutions. Cosurfactants which form viscoelastic gels, lead to the formation of largest micelles with more than 10 entangling points per micelle and very slow relaxation,  $\tau_R > 1$  s. Highly viscous solutions are formed when 3–5 entangled points are formed per micelle and  $\tau_R$  is between 1 and 10 s. Newtonian behavior of the solutions is observed at low number of entangled points ( $< 3$ ) and relaxation time  $< 1$  s.

## Acknowledgements

The study falls under the umbrellas of European network COST MP 1305 “Flowing matter” and the Horizon 2020 project “Materials Networking” (ID: 692146-H2020-eu.4.b).

## Appendix A. Supplementary data

Supplementary data associated with this article can be found, in the online version, at <http://dx.doi.org/10.1016/j.colsurfa.2017.10.018>.

## References

- [1] R. Zana, E. Kaler, *Giant Micelles Properties and Applications*, Taylor & Francis group, New York, 2007.
- [2] J. Israelachvili, *Intermolecular and Surface Forces*, 3d edition, Academic Press, 2011.
- [3] S. Ezrahi, E. Tuval, A. Aserin, Properties, main applications and perspectives of worm micelles, *Adv. Colloid Interface Sci.* 128 (–130) (2006) 77–102.
- [4] C.A. Dreiss, Wormlike micelles: where do we stand? Recent developments, linear rheology and scattering techniques, *Soft Matter* 3 (2007) 956–970.
- [5] M.E. Cates, S.J. Candau, Statics and dynamics of worm-like surfactant micelles, *J. Phys.: Condens. Matter* 2 (1990) 6869–6892.
- [6] A. Khatory, F. Lequeux, F. Kern, S.J. Candau, Linear and nonlinear viscoelasticity of semidilute solutions of wormlike micelles at high salt content, *Langmuir* 9 (1993) 1456–1464.
- [7] M.E. Cates, Reptation of living polymers: dynamics of entangled polymers in the presence of reversible chain-scission reactions, *Macromolecules* 20 (1987) 2289–2296.
- [8] M.E. Cates, Nonlinear viscoelasticity of wormlike micelles (and other reversibly breakable polymers), *J. Phys. Chem.* 94 (1990) 371–375.
- [9] M.E. Cates, S.M. Fielding, Rheology of giant micelles, *Adv. Phys.* 55 (2006) 799–879.
- [10] M.S. Turner, M.E. Cates, Linear viscoelasticity of living polymers: a quantitative probe of chemical relaxation times, *Langmuir* 7 (1991) 1590–1594.
- [11] R. Granek, Dip in  $G''(\omega)$  of polymer melts and semidilute solutions, *Langmuir* 10 (1994) 1627–1629.
- [12] A. Parker, W. Fieber, Viscoelasticity of anionic wormlike micelles: effects of ionic strength and small hydrophobic molecules, *Soft Matter* 9 (2013) 1203–1213.
- [13] D. Balzer, S. Varwig, M. Wehrauch, Viscoelasticity of personal care products, *Colloids Surf. A* 99 (1995) 233–246.
- [14] D. Acharya, H. Kunieda, Wormlike micelles in mixed surfactant solutions, *ACIS* 123 (2006) 401–413.
- [15] D.P. Acharya, T. Sato, M. Kaneko, Y. Singh, H. Kunieda, Effect of added poly (oxyethylene)dodecyl ether on the phase and rheological behavior of wormlike micelles in aqueous SDS solutions, *J. Phys. Chem. B* 110 (2006) 754–760.
- [16] K. Aramaki, S. Hoshida, S. Arima, Effect of carbon chain length of cosurfactant on the rheological properties of nonionic wormlike micellar solutions formed by a sugar surfactant and monohydroxy alcohols, *Colloids Surf., A* 366 (2010) 58–62.
- [17] K. Aramaki, S. Hoshida, S. Arima, Formation of wormlike micelles with natural-sourced ingredients (sucrose fatty acid ester and fatty acid) and a viscosity-boosting effect induced by fatty acid, *Colloids Surf., A* 396 (2012) 278–282.
- [18] S.R. Raghavan, G. Fritz, E.W. Kaler, Wormlike micelles formed by synergistic self-Assembly in mixtures of anionic and cationic surfactants, *Langmuir* 18 (2002) 3797–3803.
- [19] C. Oelschlaeger, N. Willenbacher, Mixed wormlike micelles of cationic surfactants: effect of the cosurfactant chain length on the bending elasticity and rheological properties, *Colloids Surf., A* 406 (2012) 31–37.
- [20] M. Kamada, S. Shimizu, K. Aramaki, Manipulation of the viscosity behavior of wormlike micellar gels by changing the molecular structure of added perfumes, *Colloids Surf., A* 458 (2014) 110–116.
- [21] Z. Mitrinova, S. Tcholakova, Z. Popova, N. Denkov, B. Dasgupta, K.P. Ananthapadmanabhan, Efficient control of the rheological and surface properties of surfactant solutions containing C8–C18 fatty acids as cosurfactants, *Langmuir* 29 (2013) 8255–8265.
- [22] S.E. Anachkov, P.A. Kralchevsky, K.D. Danov, G.S. Georgieva, K.P. Ananthapadmanabhan, Dislike vs. cylindrical micelles: generalized model of micelle growth and data interpretation, *J. Colloid Interface Sci.* 416 (2014) 258–273.
- [23] G.S. Georgieva, S.E. Anachkov, I. Lieberwirth, K. Koynov, P.A. Kralchevsky, Synergistic growth of giant wormlike Micelles in ternary mixed surfactant solutions: effect of octanoic acid, *Langmuir* 32 (2016) 12885–12893.
- [24] Z. Mitrinova, S. Tcholakova, N. Denkov, K.P. Ananthapadmanabhan, Role of interactions between cationic polymers and surfactants for foam properties, *Colloids and Surfaces A: Physicochem. Eng. Aspects* 489 (2016) 378–391.
- [25] D.P. Acharya, H. Kunieda, Formation of viscoelastic wormlike micellar solutions in mixed nonionic surfactant systems, *J. Phys. Chem. B* 107 (2003) 10168–10175.
- [26] F. Kern, P. Lemarchal, S.J. Candau, M.E. Cates, Rheological properties of semi-dilute and concentrated solutions of cetyltrimethylammonium bromide in the presence of potassium bromide, *Langmuir* 8 (1992) 437–440.
- [27] A. Khatory, F. Kern, F. Lequeux, J. Appell, G. Porte, N. Morie, A. Ott, W. Urbach, Entangled versus multiconnected network of wormlike micelles, *Langmuir* 9 (1993) 933–939.
- [28] R.G. Shrestha, L.K. Shrestha, T. Matsunaga, M. Shibayama, K. Aramaki, Lipophilic tail architecture and molecular structure of neutralizing agent for the controlled rheology of viscoelastic fluid in amino-based anionic surfactant system, *Langmuir* 27 (2011) 2229–2236.
- [29] N.A. Spenley, M.E. Cates, T.C.B. McLeish, Nonlinear rheology of wormlike micelles, *Phys. Rev. Letter* 71 (1993) 939–942.
- [30] M.M. Cross, Rheology of non-Newtonian fluids: a new flow equation for pseudo-plastic systems, *J. Colloid Sci.* 20 (1965) 417–437.
- [31] K. Tsujii, *Surface Activity Principles, Phenomena and Applications*, Academic press, San Diego, 1998.
- [32] S. Tzochcheva, K.D. Danov, P.A. Kralchevsky, G.S. Georgieva, A.J. Post, K.P. Ananthapadmanabhan, Solubility limits and phase diagrams for fatty alcohols in anionic (SLES) and zwitterionic (CAPB) micellar surfactant solutions, *J. Colloid Interface Sci* 449 (2015) 46–61.
- [33] S.S. Tzochcheva, P.A. Kralchevsky, K.D. Danov, G.S. Georgieva, A.J. Post, K.P. Ananthapadmanabhan, Solubility limits and phase diagrams for fatty acids in anionic (SLES) and zwitterionic (CAPB) micellar surfactant solutions, *J. Colloid Interface Sci* 369 (2012) 274–286.
- [34] R. Kumar, G.C. Kalur, L. Ziserman, D. Danino, S.R. Raghavan, Wormlike micelles of a C22-Tailed zwitterionic betaine surfactant: from viscoelastic solutions to elastic gels, *Langmuir* 23 (2007) 12849–12856.
- [35] H.A. Barnes, J.F. Hutton, K. Walters, *An Introduction to Rheology*, Elsevier Scientific publishers B.V., Amsterdam, 1989.
- [36] M. Doi, S.F. Edwards, *The Theory of Polymer Dynamics*, Clarendon Press, Oxford, 1986.
- [37] Z. Mitrinova, S. Tcholakova, K. Golemanov, N. Denkov, M. Vethamuthu, K.P. Ananthapadmanabhan, Surface and foam properties of SLES + CAPB + fatty acid mixtures: effect of pH for C12–C16 acids, *Colloids Surf. A: Physicochem. Eng. Asp.* 438 (2013) 186–198.
- [38] R. Granek, M.E. Cates, Stress relaxation in living polymers: results from a Poisson renewal model, *J. Chem. Phys.* 96 (1992) 4758–4767.
- [39] L.J. Magid, Z. Han, Z. Li, P.D. Butler, Tuning the contour lengths and persistence lengths of cationic micelles: the role of electrostatics and specific ion binding, *J. Phys. Chem. B* 104 (2000) 6717–6727.
- [40] P. Ruoff, Linear free energy relationships An information theoretic view. *Z. Phys. Chemie, Leipzig* 3 (1984) 433–440.
- [41] Y. Simon-Manso, Linear free-Energy relationships and the density functional theory: an analog of the hammett equation, *J. Phys. Chem. A* 109 (2005) 2006–2011.